JACS
JOURNAL OF THE AMERICAN CHEMICAL SOCIETY
Article
pubs.acs.org/JACS

A Liquid Junction Photoelectrochemical Solar Cell Based on p-Type $MeNH_3PbI_3$ Perovskite with 1.05 V Open-Circuit Photovoltage

Hsien-Yi Hsu,[†] Li Ji,[†,‡] Hyun S. Ahn,[†] Ji Zhao,[†] Edward T. Yu,[‡] and Allen J. Bard*[,†]

[†]Center for Electrochemistry, Department of Chemistry, and [‡]Microelectronics Research Center, Department of Electrical and Computer Engineering, The University of Texas at Austin, Austin, Texas 78712, United States

Supporting Information

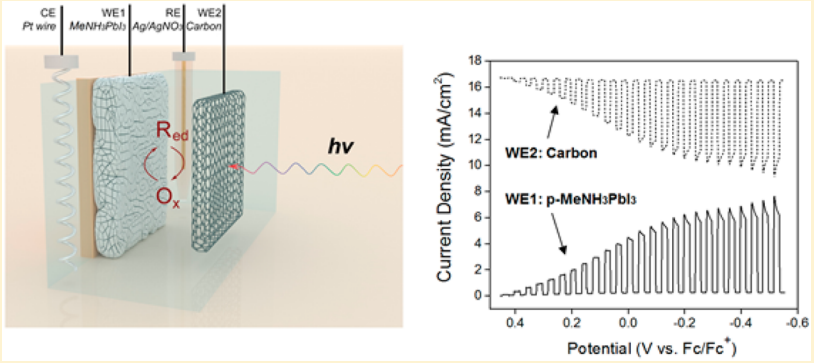

ABSTRACT: A liquid junction photoelectrochemical (PEC) solar cell based on p-type methylammonium lead iodide (p-$MeNH_3PbI_3$) perovskite with a large open-circuit voltage is developed. $MeNH_3PbI_3$ perovskite is readily soluble or decomposed in many common solvents. However, the solvent dichloromethane (CH_2Cl_2) can be employed to form stable liquid junctions. These were characterized with photoelectrochemical cells with several redox couples, including I_3^-/I^-, Fc/Fc^+, $DMFc/DMFc^+$, and $BQ/BQ^{\bullet-}$ (where Fc is ferrocene, DMFc is decamethylferrocene, BQ is benzoquinone) in CH_2Cl_2. The solution-processed $MeNH_3PbI_3$ shows cathodic photocurrents and hence p-type behavior. The difference between the photocurrent onset potential and the standard potential for $BQ/BQ^{\bullet-}$ is 1.25 V, which is especially large for a semiconductor with a band gap of 1.55 eV. A PEC photovoltaic cell, with a configuration of p-$MeNH_3PbI_3/CH_2Cl_2$, BQ (2 mM), $BQ^{\bullet-}$ (2 mM)/carbon, shows an open-circuit photovoltage of 1.05 V and a short-circuit current density of 7.8 mA/cm^2 under 100 mW/cm^2 irradiation. The overall optical-to-electrical energy conversion efficiency is 6.1%. The PEC solar cell shows good stability for 5 h under irradiation.

INTRODUCTION

The organometallic halide perovskite has attracted tremendous attention due to impressive features, including its direct band gap of ~1.55 eV, high absorption coefficient, ambipolar charge-carrier mobilities, long exciton lifetimes/diffusion length, and low exciton binding energy.[1−6] Perovskite materials have been widely used as sensitizers with TiO_2 and other metal oxides and bulk heterojunction solar cells.[7,8] In 2009, Miyasaka's group[9] first developed $MeNH_3PbX_3$ (X = I, Br) perovskite sensitized solar cells based on mesoporous TiO_2 photoanodes. However, the power conversion efficiencies (PCEs) for $MeNH_3PbI_3$ and $MeNH_3PbBr_3$ were initially as low as 3.81% and 3.13%, respectively. Later, several milestones in PCE enhancement were achieved by the innovation of cell fabrication technique. For example, Snaith's group[7] fabricated a solid-state device (FTO/PEDOT:PSS/$MeNH_3PbI_{3-x}Cl_x$/PCBM/TiO_x/Al) as a planar heterojunction, and its PCE was promoted to 10% and up to 6.5% for the same configuration on an indium-doped tin oxide (ITO)-coated plastic foil. Afterward, a solution-processed perovskite solid-state solar cell consisting of a bilayer architecture and $MeNH_3Pb(I_{1-x}Br_x)_3$ perovskites was proposed by Seok's group.[8] They demonstrated that the stability of $MeNH_3PbI_3$ perovskites was greatly improved by the substitution of 10−15 mol % Br^- for I^-, while maintaining the performance.[10] When the perovskite was deposited using a mixture of γ-butyrolactone (GBL) and dimethyl sulfoxide (DMSO), followed by a toluene drip while being spun, extremely uniform and dense layers were formed. A fully solution processed perovskite solid-state solar cell with this solvent-engineering technique can deliver up to a 16.2% PCE. Furthermore, Nie's group discovered a solution-based hot-casting technique to achieve ~18% solid-state solar cell efficiency based on millimeter-scale crystalline grains, with a relatively small variability (~2%) in the overall PCE from one solar cell to another.[11] Recently, a higher PCE of 19.3% in solid-state solar cells was reached with polyethylenimine ethoxylate (PEIE) modified ITO and yttrium-doped TiO_2 (Y−TiO_2),[12] because PEIE-modified ITO can reduce the work function of ITO[13] and Y−TiO_2, the electron port layer

Received: September 16, 2015
Published: November 2, 2015

DOI: 10.1021/jacs.5b09758
J. Am. Chem. Soc. 2015, 137, 14758−14764

Table 1. Summary of the Stability for $MeNH_3PbI_3$ Perovskites and Solubility of Redox Couples in a Series of Solvents

			solubility			
solvent	dielectric constant	stability of $MeNH_3PbI_3$	I_3^-/I^-	Fc/Fc^+	$DMFc/DMFc^+$	$BQ/BQ^{\bullet-}$
dimethyl sulfoxide	46.7	N[a]	V[a]	V	V	V
acetonitrile	37.5	N	V	V	V	V
dichloromethane	8.93	Y[a]	V	V	V	V
tetrahydrofuran	7.58	N	V	V	V	V
ethyl acetate	6.02	N	V	V	V	V
chloroform	4.81	Y	X[a]	V	V	V
toluene	2.38	Y	X	X	X	X

[a]N means that the stability of $MeNH_3PbI_3$ in this solvent is not good; Y means that the stability of $MeNH_3PbI_3$ in this solvent is good; V means that the solubility of this redox couple in this solvent is good; X means that the solubility of this redox couple in this solvent is not good.

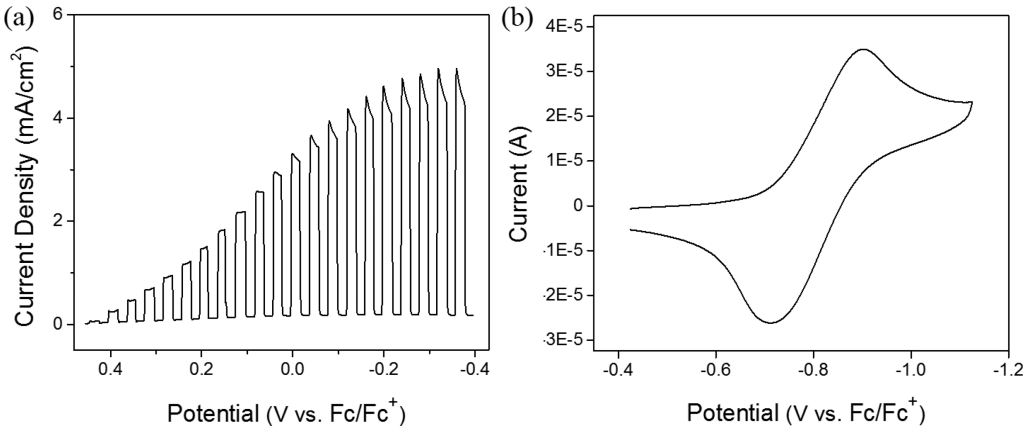

Figure 1. Voltammetric curves of p-$MeNH_3PbI_3$ and C in CH_2Cl_2 containing 2 mM BQ, 2 mM $BQ^{\bullet-}$, and 0.1 M $TBAPF_6$ (supporting electrolyte). Light source, 100 mW/cm^2 xenon lamp. Scan rate = 50 mV/s. (a) LSV characteristics under chopped illumination on p-$MeNH_3PbI_3$. (b) Cyclic voltammogram at C electrodes.

(ETL), and can enhance the extraction and transport of electrons.

A liquid junction PEC cell with $MeNH_3PbI_3$ is of interest for several reasons. A liquid junction solar cell produces a photoactive junction simply upon immersing the semiconductor in solution, which simplifies the assembly of the cell. More importantly, it also allows one to do combinatorial screening. In this report, we therefore develop a liquid junction PEC solar cell based on p-type $MeNH_3PbI_3$ (p-$MeNH_3PbI_3$) using a reticulated vitreous carbon as the counter electrode. Because $MeNH_3PbI_3$ is moisture-sensitive and can be dissolved in most organic solvents, identification of a suitable organic solvent is mandatory. Here, we identify and characterize the appropriate organic solvents for $MeNH_3PbI_3$ perovskites that enable both fundamental studies and an operating PEC solar cell. We explore electrochemical behaviors and PEC effects on p-$MeNH_3PbI_3$ electrodes. The efficiencies of these PEC cells strongly depend on the nature of the redox couples in solution.

EXPERIMENTAL SECTION

Preparation of p-$MeNH_3PbI_3$ Film. p-$MeNH_3PbI_3$ was drop-cast on fluorine-doped tin oxide (FTO) glass substrates from *N*,*N*-dimethylformamide (DMF) (Alfa Aesar) solution with an equimolar mixture of $MeNH_3I$ and PbI_2. $MeNH_3I$ was synthesized by stirring 27.86 mL of methylamine (2 M in methanol, Alfa Aesar) and 30 mL of hydroiodic acid (57 wt % in water, Alfa Aesar) in a 250 mL round bottomed flask in an ice bath under an argon atmosphere for 3 h. After the reaction, the solvent was evaporated using a rotary evaporator. A white powder, methylammonium iodide ($MeNH_3I$), was washed with diethyl ether by stirring the solution for 30 min, which was repeated three times, and then finally dried at 60 °C in a vacuum oven for 24 h.[14] The synthesized $MeNH_3I$ white powder was mixed with PbI_2 (Alfa Aesar) at 1:1 mol ratio in DMF at 100 °C for 1 h.[15]

Photoelectrochemical Measurements. The photoactivity of p-$MeNH_3PbI_3$ was measured in a photoelectrochemical cell. The prepared films were used as working electrodes (0.27 cm^2) exposed to electrolyte solution and irradiation. All measurements were carried out in a borosilicate glass cell with a carbon counter electrode and Ag/$AgNO_3$ reference electrode (a silver wire immersed in 0.01 M silver nitrate in MeCN connected to the cell via a 0.10 M $TBAPF_6$ in CH_2Cl_2 salt bridge, as shown in Figure S-2 of the Supporting Information (SI). All potentials are reported vs Fc/Fc^+ in CH_2Cl_2. UV−vis light was irradiated through the electrolyte solution using full output of the Xe lamp with an incident light intensity of about 100 mW/cm^2. The supporting electrolyte was 0.1 M tetrabutylammonium hexafluorophosphate ($TBAPF_6$) in CH_2Cl_2. The IPCE was measured through a monochromator (Photon Technology International, Birmingham, NJ) in combination with a power meter (model 1830-C, Newport, Irvine, CA) and a silicon detector (model 818-UV, Newport, Irvine, CA). Electrochemical impedance spectroscopy (EIS) was performed using an Autolab instrument (PGSTAT30/FRA2) to obtain the Mott−Schottky plot at frequencies of 500, 2000, and 5000 Hz and peak-to-peak amplitude of 5 mV at each potential.

Instruments. A CH Instruments model 760E electrochemical analyzer (Austin, TX) was used as a potentiostat for the experiments with the thin film electrodes. Illumination was with a xenon lamp (XBO 150 W, Osram) at full output for UV−visible irradiation. Glancing incidence angle X-ray diffraction (XRD) measurements were performed by using a D8 ADVANCE (Bruker, Fitchburg, WI) instrument equipped with a Cu Kα radiation source where the incident angle was 0.4°. The film thickness was measured by scanning electron microscopy (SEM, Quanta 650 FEG, FEI Co., Inc., Hillsboro, OR). In the solar cell measurements, current (I) and voltage (V) readings were taken between the working electrode and the carbon counter electrode

DOI: 10.1021/jacs.5b09758
J. Am. Chem. Soc. 2015, 137, 14758−14764

without external power source using a Keithley model 2400 electrometer and a xenon lamp solar simulator (Newport) equipped with an AM1.5G filter.

RESULTS AND DISCUSSION

Solvents and Redox Couples for p-$MeNH_3PbI_3$. $MeNH_3PbI_3$ perovskites are extremely sensitive to moisture[16] and unstable in polar solvents.[17] We then examined a number of stable solvents for $MeNH_3PbI_3$ in consideration of the polarity and dielectric constant, as depicted in Table 1. $MeNH_3PbI_3$ perovskites dissolved completely in common solvents, such as dimethyl sulfoxide (DMSO), acetonitrile (MeCN), tetrahydrofuran (THF), and ethyl acetate (EA). Thus, lower dielectric constant solvents were considered and investigated. A few low dielectric constant solvents, including dichloromethane (CH_2Cl_2), chloroform ($CHCl_3$), and toluene, are possible candidates for $MeNH_3PbI_3$ PEC studies with good stability. To study the fundamental electrochemical and PEC properties, soluble redox couples have to be determined in these systems. The standard potentials of several redox couples, such as I_3^-/I^-, Fc/Fc^+, $DMFc/DMFc^+$, and $BQ^{\bullet-}/BQ$, should be within the band gap of p-$MeNH_3PbI_3$. They were investigated, and the results are summarized in Table 1. Due to its relatively higher dielectric constant and stability for $MeNH_3PbI_3$ perovskites, CH_2Cl_2 is considered as the solvent for further exploration of this perovskite.

Current−Potential Behavior. Cyclic voltammograms (CV) were obtained for the various redox couples in 0.1 M $TBAPF_6$ at a glassy carbon electrode (diameter = 3 mm). A typical CV for 2 mM BQ, 2 mM $BQ^{\bullet-}$ is given in Figure 1b. This wave shows peak splitting with the first wave at −0.90 V and the second at −0.70 V (formal potential = −0.80 vs Fc/Fc^+). Under chopped illumination, a typical linear sweep voltammogram (LSV) shows that a significant cathodic current flows with the onset at about 0.45 V vs Fc/Fc^+, which should be about the valence band edge or flat band potential (E_{fb}). The photocurrent at potentials more positive than those for reduction at the C electrode (Figure 1a) represent conversion of radiant energy to electrical energy. The PEC curve at the p-$MeNH_3PbI_3$ shows significant uncompensated resistance, about 1986.8 Ω in Figure S-2 (SI). From E_{fb} and the potential for the oxidation of $BQ^{\bullet-}$ on a C electrode, we predict that a PEC solar cell based on p-$MeNH_3PbI_3$ photocathode and a carbon anode in a $BQ^{\bullet-}/BQ$ solution would show an open circuit photovoltage of more than 1 V and a good energy conversion efficiency. The individual current−potential behaviors of p-$MeNH_3PbI_3$ containing different redox couples, I_3^-/I^-, Fc/Fc^+, and $DMFc/DMFc^+$, were also investigated, and the voltammetric data and onset potential of photocurrent are displayed in Table 2, which shows that the difference between the onset potential for the photocurrent (E_{on}) and the standard potential of the redox couple (E^o), ΔE, is generally about 0.25−1.25 V, relatively more dependent on E^o for the redox couple. These results suggest that the simple idealized model for a semiconductor/solution interface can be applied to explain the behavior.[18] During the CV and PEC measurements, we found that p-$MeNH_3PbI_3$ can be dissolved/decomposed in the iodide liquid electrolyte in CH_2Cl_2, in agreement with the previous reported results in EA.[19] The I_3^-/I^- system is thus unsuitable for application as a PEC solar cell. Furthermore, ΔE of a Fc/Fc^+ system is too small to have an acceptable open-circuit photovoltage. Clearly, from its position within the band gap of the $MeNH_3PbI_3$ (Figure 2b), $BQ^{\bullet-}/BQ$ is the best candidate redox couple for a PEC cell.

Table 2. Voltammetric Data and Onset Potential of Photocurrent[a]

redox couple	E^o, V vs Fc/Fc^+ [a]	E_{on}, V vs Fc/Fc^+ [b]	$\Delta E = E_{on} - E^o$, V
I_3^-/I^-	−0.15	0.25	0.40
Fc/Fc^+	0.00	0.25	0.25
$DMFc/DMFc^+$	−0.43	0.15	0.58
$BQ^{\bullet-}/BQ$	−0.80	0.45	1.25

[a] E^0 = the formal potentials (V vs Fc/Fc^+). [b] The onset potential of photocurrent E_{on} here is defined as the potential at which 1% of the limiting or maximal photocurrent is observed.

Capacitance Measurements and Energy Level Diagram. Knowledge of the energy levels of the valence and the conduction bands (E_v and E_c) of the semiconductor electrode with reference to solution energy levels is helpful in selecting useful redox couples for maximizing the performance of a PEC solar cell. In addition to estimation from the potential for the onset of photocurrent, the valence band edge and E_{fb} can also be determined by capacitance measurements [Mott−Schottky (MS) plots], i.e., capacitance of the semiconductor/electrolyte interface as a function of the applied potential. This capacitance is assumed to be the semiconductor space-charge capacitance, where E_{fb} and the acceptor density (N_A) can be estimated from the potential-axis intercept and the slope of the MS plot.[20] MS analysis of the p-$MeNH_3PbI_3$ electrode in CH_2Cl_2/0.1 M $TBAPF_6$ for frequencies of 500, 2000, and 5000 Hz is shown in Figure 2a. The x-intercepts of the solid lines manifest that a E_{fb} potential appears to be ∼0.46 ± 0.01 V vs Fc/Fc^+, which is close to the onset photopotential of p-$MeNH_3PbI_3$ in a $BQ^{\bullet-}/BQ$ system (onset potential = 0.45 vs Fc/Fc^+). Although some frequency dispersion is seen in the capacitance, we can report an approximate average acceptor density of 9×10^{15} cm^{-3} based on a dielectric constant of 6.5 determined from measurements using $MeNH_3PbI_3$ powders.[21] The energy levels of the p-$MeNH_3PbI_3$/electrolyte interface are shown in Figure 2b.

Light Intensity Limited Performance and Detection of Products. In the operation of a liquid junction PEC cell, the current can be limited by the light intensity or by the mass transfer of the reactant to the semiconductor surface. In general, for the optimum operation, it is required that the concentration of the reactant must be sufficiently large that mass transfer does not limit the current. The LSVs of a p-$MeNH_3PbI_3$ cathode in $BQ^{\bullet-}/BQ$ electrolyte with different concentrations (1, 2, 5, and 10 mM each) were investigated, as depicted in Figure 3a. The photocurrent densities at −0.36 V vs Fc/Fc^+ were plotted at various concentrations (Figure 3b). The performance of the PEC reaches a plateau as the concentration of the $BQ^{\bullet-}/BQ$ system is higher than 2 mM. Then the LSVs of a p-$MeNH_3PbI_3$ perovskite in a CH_2Cl_2 solution of 2 mM $BQ^{\bullet-}$ and 2 mM BQ electrolytes were monitored at different light intensities (40, 60, 100, and 150 mW/cm^2), as shown in Figure 3c. The photocurrent density increases linearly with increasing illumination intensity (Figure 3d). Therefore, we demonstrate that the PEC of a p-$MeNH_3PbI_3$ semiconductor in the 2 mM $BQ^{\bullet-}/BQ$ system is light intensity limited.

Figure 4 shows the scheme of a measurement setup, which involves the simultaneous potential control of two working electrodes for the generation and detection of reduced species on the first working electrode (WE1), which consists of p-

DOI: 10.1021/jacs.5b09758
J. Am. Chem. Soc. 2015, 137, 14758−14764

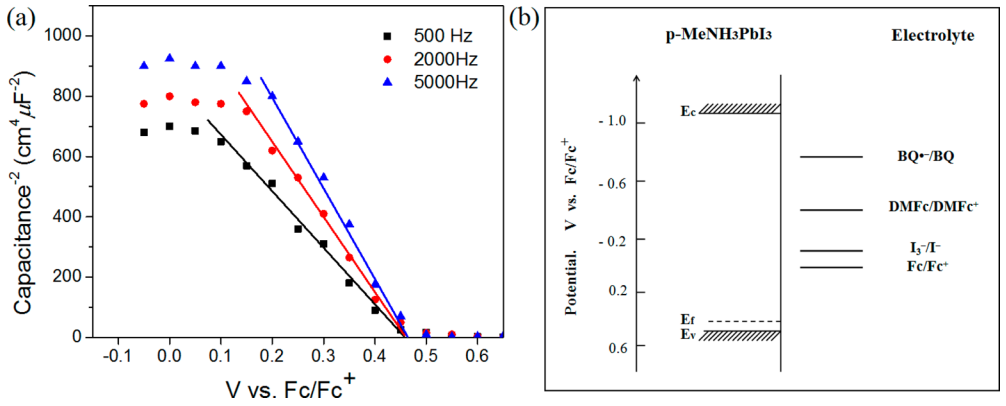

Figure 2. (a) Mott–Schottky plot of p-$MeNH_3PbI_3$ in CH_2Cl_2 containing 0.1 M $TBAPF_6$ supporting electrolyte at 500, 2000, and 5000 Hz. The solid lines are linear fits to the experimental data. (b) Schematic diagram of the energy levels at the p-$MeNH_3PbI_3$/electrolyte interface. E_c, E_f, and E_v denote the potentials of the conduction band edge, the Fermi energy, and the valence band edge of p-$MeNH_3PbI_3$, respectively.

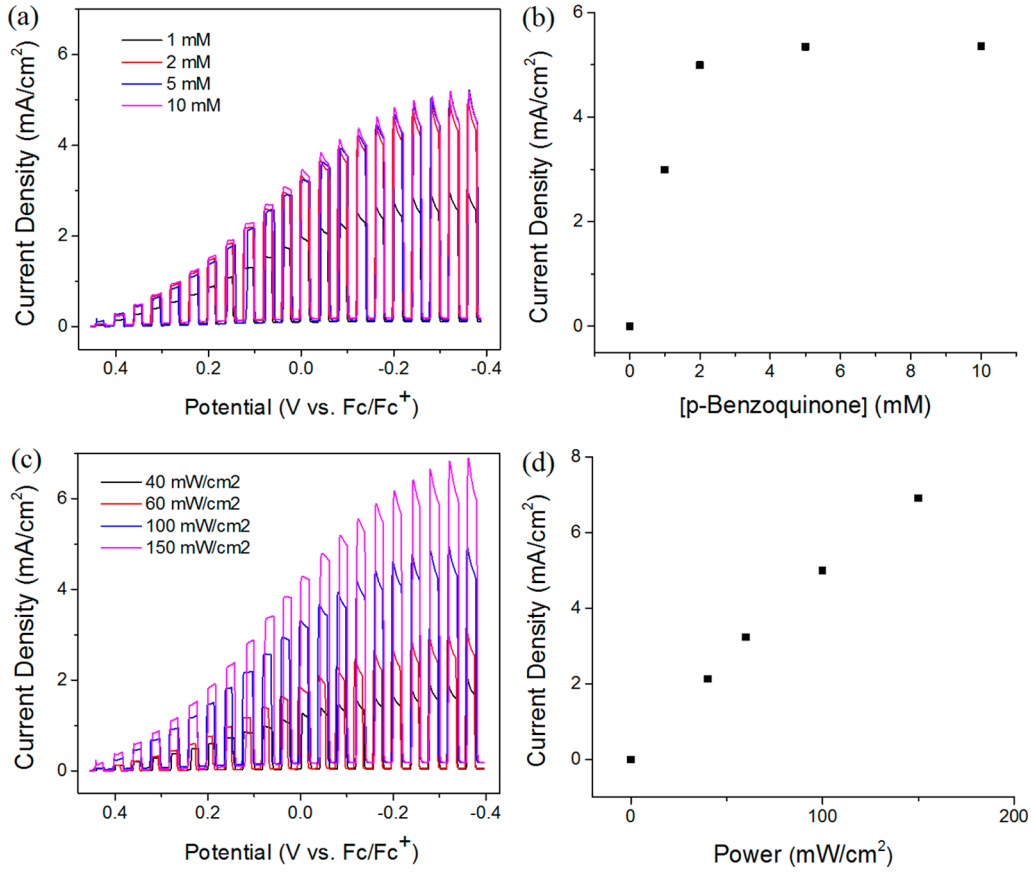

Figure 3. (a) The chopped light LSV at different concentrations (1, 2, 5, and 10 mM). (b) The photocurrent at −0.36 V vs Fc/Fc^+ with different concentrations (1, 2, 5, and 10 mM). (c) The LSV with different light intensities (40, 60, 100, and 150 mW/cm^2). (d) The photocurrent at −0.36 V vs Fc/Fc^+ with different light intensities (40, 60, 100, and 150 mW/cm^2) for a p-$MeNH_3PbI_3$ cathode in $BQ^{\bullet-}$/BQ electrolyte under illumination from a 100 mW/cm^2 Xe lamp.

$MeNH_3PbI_3$ perovskites on the FTO substrate. At the same time, a potential is applied to the reticulated vitreous carbon as a second working electrode (WE2) to produce an oxidized mediator species O_x at a diffusion-limited rate from a reduced species (R_{ed}), which is produced by WE1 in the electrolyte. In this measurement, the p-$MeNH_3PbI_3$ perovskites were irradiated at the front side because p-$MeNH_3PbI_3$ is too thick (~30 μm) to produce efficient charge carriers under irradiation from the back. Figure 5 shows the voltammetric curves of WE1 and WE2. Under irradiation of 100 mW/cm^2, p-$MeNH_3PbI_3$ WE1 displayed p-type behavior and was photoactive in the reduction of BQ, spanning a potential range of about 0.45 to −0.55 V vs Fc/Fc^+. The photocurrent density could be increased up to 7.6 mA/cm^2 under these conditions, as the optical path through the solution to the photocathode was minimized. Species $BQ^{\bullet-}$ diffused from the p-$MeNH_3PbI_3$, and it collected and oxidized at the reticulated vitreous carbon (WE2) held at a constant potential, where oxidation is diffusion-controlled. The anodic photocurrent we detected is assigned to the oxidation of $BQ^{\bullet-}$. The current density of WE1

DOI: 10.1021/jacs.5b09758
J. Am. Chem. Soc. 2015, 137, 14758–14764

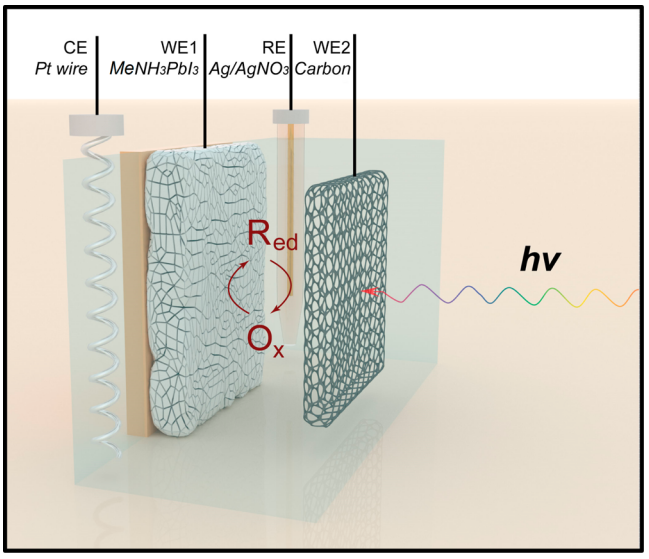

Figure 4. Schematic illustration of the photoelectrochemical test of a p-$MeNH_3PbI_3$ photocathode in a PEC cell using a standard four-electrode system. In this measurement, the reference electrode (RE) and counter electrode (CE) were placed at both sides of the p-$MeNH_3PbI_3$ photocathode. The photocathode is front illuminated on the perovskite side. WE1, p-$MeNH_3PbI_3$; WE2, reticulated vitreous carbon; RE, $Ag/AgNO_3$; CE, Pt wire; 0.1 M $TBAPF_6$; 2 mM BQ; 2 mM $BQ^{\bullet-}$; scan rate, 10 mV/s.

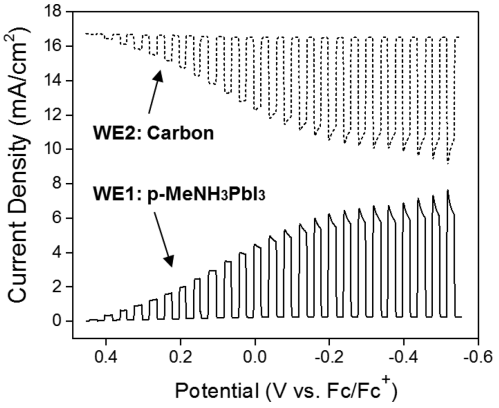

Figure 5. Voltammetric curves of p-$MeNH_3PbI_3$ (WE1, black curve) and C (WE2, black short-dashed curve) in CH_2Cl_2 containing 2 mM BQ, 2 mM $BQ^{\bullet-}$, and 0.1 M $TBAPF_6$ (supporting electrolyte). The potential of WE1 was swept from 0.45 to −0.55 V vs Fc/Fc^+ at a scan rate of 10 mV/s. WE2 was held at a constant potential (approximately −0.60 V vs Fc/Fc^+). The incident light intensity at the electrode surface was 100 mW/cm^2.

and WE2 are about the same at steady state, demonstrating the high stability of the reactants, so that a p-$MeNH_3PbI_3$ and C counter electrode in $BQ^{\bullet-}$/BQ CH_2Cl_2 solution is promising as a two-electrode liquid junction solar cell.

PEC Solar Cells. The LSV behavior can be used as a guide for the construction of PEC photovoltaic cells, where the open-circuit potential of the semiconductor ideally (in the absence of recombination) approaches ΔV. The photocurrents found in the LSV experiments with p-$MeNH_3PbI_3$ were relatively efficient, and the experimental results between actual two-electrode photovoltaic cells are also of interest because they clearly show that the responses are not caused by conductivity changes under illumination. The PEC behavior of these electrodes was investigated in a cell. The following cell was prepared: p-$MeNH_3PbI_3/CH_2Cl_2$, $TBAPF_6$ (0.1 M), $BQ^{\bullet-}$ (2 mM), BQ (2 mM)/C. The p-$MeNH_3PbI_3$ photocathode (4 cm^2) and the reticulated vitreous carbon (6.25 cm^2) counter electrode were spaced about 0.30 mm apart with a Teflon gasket, with the p-$MeNH_3PbI_3$ electrode about <1 mm away from the cell window. The cell shows the following overall characteristics. In the ideal model of the semiconductor/interface, the open-circuit photovoltage is similar to the difference between the flat-band potential of a semiconductor electrode (E_{fb}) and the formal potential of a redox couple (E^o),[18] which is consistent with this study of p-$MeNH_3PbI_3$ in CH_2Cl_2 solutions. From the result in Figure 6, at a light flux of

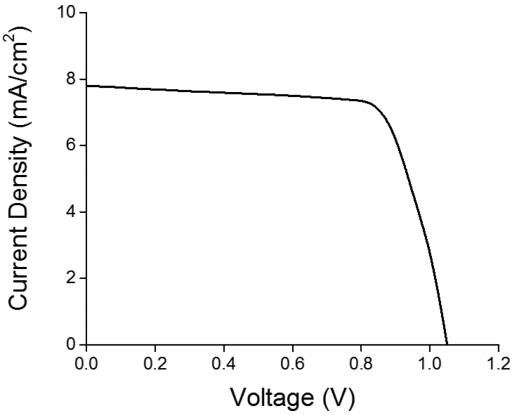

Figure 6. Steady-state current density−voltage relation for a p-$MeNH_3PbI_3$/BQ (2 mM), $BQ^{\bullet-}$ (2 mM)/C PEC cell under irradiation with a 100 mW/cm^2 xenon lamp focused onto the photoelectrode. The optical path through the solution was about 0.3 mm.

100 mW/cm^2, the overall optical-to-electrical energy conversion efficiency, uncorrected for absorption and reflectivity losses, was ~6.1%. This relatively high value can probably be attributed to slow recombination processes and long electron−hole diffusion length (over 100 nm)[22] both within the bulk p-$MeNH_3PbI_3$ and at the interface. To decrease the light adsorption by this intensely colored species, the $BQ^{\bullet-}$/BQ solutions were kept at a low concentration. The performances of the liquid junction PEC cell in $BQ^{\bullet-}$/BQ electrolyte with different concentrations (1, 2, 5, and 10 mM each) were then studied. The optical-to-electrical energy conversion efficiencies in the 2, 5, and 10 mM $BQ^{\bullet-}$/BQ system were all around 6.0%. The other liquid junction PEC cell, p-$MeNH_3PbI_3/CH_2Cl_2$, $TBAPF_6$ (0.1 M), DMFc (2 mM), $DMFc^+$ (2 mM)/C, was also investigated. The open-circuit photovoltage was 0.45 V, the short-circuit photocurrent density was 7.5 mA/cm^2, and the fill factor was 0.68. The open-circuit voltage is also slightly lower than the value predicted from voltammetric measurements conducted with 2 mM DMFc and 2 mM $DMFc^+$ solutions. Clearly, the liquid junction solar cell with the $BQ^{\bullet-}$/BQ system is better than that with the $DMFc/DMFc^+$ system. Furthermore, the photocurrent for the p-$MeNH_3PbI_3$ in the 2 mM $BQ^{\bullet-}$/BQ system was measured as a function of wavelength over the range from 300 to 800 nm using a Xe lamp. The incident photon-to-electron conversion efficiencies (IPCEs) were calculated and are plotted in Figure 7, and they reach a maximum of 55% at 380 nm and gradually declined at longer wavelength. Integration of the IPCE spectra gives a

DOI: 10.1021/jacs.5b09758
J. Am. Chem. Soc. 2015, 137, 14758−14764

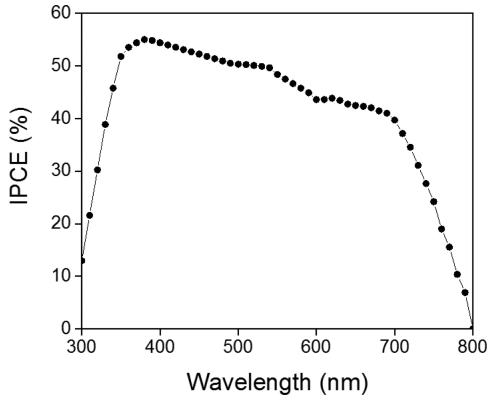

Figure 7. IPCE spectrum for the p-$MeNH_3PbI_3$ perovskite PEC solar cell.

current density of 7.5 mA/cm^2, and there is good agreement with the current density measured using the solar simulator. The photocurrent as a function of time is shown in Figure 8.

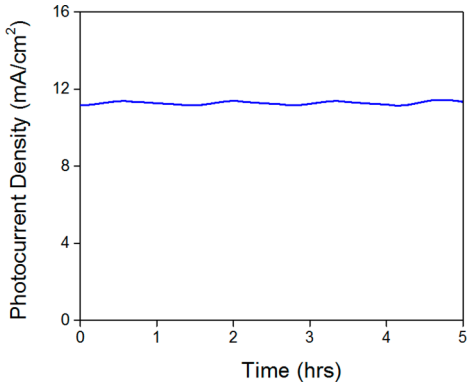

Figure 8. Time dependence of the photocurrent of a p-$MeNH_3PbI_3$/BQ (2 mM), $BQ^{\bullet-}$ (2 mM)/carbon PEC cell at 0.5 V. The p-$MeNH_3PbI_3$ photoelectrode was irradiated by a 150 mW/cm^2 Xe lamp. The optical path through the solution was about 0.3 mm.

The photocurrent was stable for 5 h, at which time the experiment was terminated under irradiation at the higher power intensity (150 mW/cm^2). The long-term stability of p-type $MeNH_3PbI_3$ liquid junction PEC solar cells was also tested for 50 h. We observed that the initial photocurrent density was decreased by 50% at ~22 h, as depicted in Figure S-4 (SI). The cause of this deactivation is under investigation.

SUMMARY AND CONCLUSION

Liquid junction PEC cells with p-type $MeNH_3PbI_3$ perovskites have been constructed. To optimize performance and improve efficiency, experiments examining the solubility, electrochemistry, and photoelectrochemistry of p-$MeNH_3PbI_3$ with several redox couples were investigated. The PEC cell p-$MeNH_3PbI_3$/BQ (2 mM), $BQ^{\bullet-}$ (2 mM)/C shows about 6.1% optical to electrical energy conversion efficiency with an open-circuit voltage of 1.05 V, a short-circuit current density of 7.8 mA/cm^2, and relatively higher fill factor (FF = 74%) under irradiation with 100 mW/cm^2. In addition, the liquid junction solar cell has some advantages over solid-state ones in terms of ease of fabrication. The use of liquid electrolytes allows easy combinatorial synthesis and screening of new perovskite materials in arrays and the testing of various dopants on them. Such studies are underway for discovering and optimizing new perovskite materials to promote the efficiency of solar energy applications.

ASSOCIATED CONTENT

Supporting Information

The Supporting Information is available free of charge on the ACS Publications website at DOI: 10.1021/jacs.5b09758.

Materials list, XRD for $MeNH_3PbI_3$, diagram for the reference electrode, and uncompensated resistance and long-term stability test for $MeNH_3PbI_3$ (PDF)

AUTHOR INFORMATION

Corresponding Author

*ajbard@mail.utexas.edu

Author Contributions

H.-Y.H. and L.J. contributed equally to this work.

Notes

The authors declare no competing financial interests.

ACKNOWLEDGMENTS

The authors gratefully acknowledge the support of U.S. Department of Energy (Grant DE-SC0002219) and the Welch Foundation (F-0021).

REFERENCES

(1) Hao, F.; Stoumpos, C. C.; Chang, R. P. H.; Kanatzidis, M. G. *J. Am. Chem. Soc.* **2014**, *136*, 8094.
(2) Cao, D. H.; Stoumpos, C. C.; Malliakas, C. D.; Katz, M. J.; Farha, O. K.; Hupp, J. T.; Kanatzidis, M. G. *APL Mater.* **2014**, *2*, 091101.
(3) Etgar, L.; Gao, P.; Xue, Z.; Peng, Q.; Chandiran, A. K.; Liu, B.; Nazeeruddin, M. K.; Grätzel, M. *J. Am. Chem. Soc.* **2012**, *134*, 17396.
(4) Kagan, C.; Mitzi, D.; Dimitrakopoulos, C. *Science* **1999**, *286*, 945.
(5) Kojima, A.; Ikegami, M.; Teshima, K.; Miyasaka, T. *Chem. Lett.* **2012**, *41*, 397.
(6) Gao, P.; Gratzel, M.; Nazeeruddin, M. K. *Energy Environ. Sci.* **2014**, *7*, 2448.
(7) Docampo, P.; Ball, J. M.; Darwich, M.; Eperon, G. E.; Snaith, H. J. *Nat. Commun.* **2013**, *4*, 2761.
(8) Jeon, N. J.; Noh, J. H.; Kim, Y. C.; Yang, W. S.; Ryu, S.; Seok, S. I. *Nat. Mater.* **2014**, *13*, 897.
(9) Kojima, A.; Teshima, K.; Shirai, Y.; Miyasaka, T. *J. Am. Chem. Soc.* **2009**, *131*, 6050.
(10) Noh, J. H.; Im, S. H.; Heo, J. H.; Mandal, T. N.; Seok, S. I. *Nano Lett.* **2013**, *13*, 1764.
(11) Nie, W.; Tsai, H.; Asadpour, R.; Blancon, J.-C.; Neukirch, A. J.; Gupta, G.; Crochet, J. J.; Chhowalla, M.; Tretiak, S.; Alam, M. A. *Science* **2015**, *347*, 522.
(12) Zhou, H.; Chen, Q.; Li, G.; Luo, S.; Song, T.-b.; Duan, H.-S.; Hong, Z.; You, J.; Liu, Y.; Yang, Y. *Science* **2014**, *345*, 542.
(13) Zhou, Y.; Fuentes-Hernandez, C.; Shim, J.; Meyer, J.; Giordano, A. J.; Li, H.; Winget, P.; Papadopoulos, T.; Cheun, H.; Kim, J. *Science* **2012**, *336*, 327.
(14) Im, J.-H.; Lee, C.-R.; Lee, J.-W.; Park, S.-W.; Park, N.-G. *Nanoscale* **2011**, *3*, 4088.
(15) Zhao, Y.; Zhu, K. *J. Phys. Chem. C* **2014**, *118*, 9412.
(16) Niu, G.; Guo, X.; Wang, L. *J. Mater. Chem. A* **2015**, *3*, 8970–8980.
(17) Grätzel, M. *Nat. Mater.* **2014**, *13*, 838.
(18) Fan, F.-R. F.; Bard, A. J. *J. Am. Chem. Soc.* **1980**, *102*, 3677–3683.
(19) Fan, J.; Jia, B.; Gu, M. *Photonics Res.* **2014**, *2*, 111.
(20) Nagasubramanian, G.; Gioda, A. S.; Bard, A. J. *J. Electrochem. Soc.* **1981**, *128*, 2158.

DOI: 10.1021/jacs.5b09758
J. Am. Chem. Soc. 2015, 137, 14758–14764

(21) Hirasawa, M.; Ishihara, T.; Goto, T.; Uchida, K.; Miura, N. *Phys. B* **1994**, *201*, 427.
(22) Stranks, S. D.; Eperon, G. E.; Grancini, G.; Menelaou, C.; Alcocer, M. J.; Leijtens, T.; Herz, L. M.; Petrozza, A.; Snaith, H. J. *Science* **2013**, *342*, 341.

DOI: 10.1021/jacs.5b09758
J. Am. Chem. Soc. 2015, 137, 14758−14764